Progress In Electromagnetics Research, Vol. 111, 381–406, 2011

A STUDY OF AN INVERSION MODEL FOR SEA ICE THICKNESS RETRIEVAL IN ROSS ISLAND, ANTARCTICA

Y. J. Lee

Universiti Tunku Abdul Rahman
Malaysia

W. K. Lim

Multimedia University
Malaysia

H. T. Ewe

Universiti Tunku Abdul Rahman
Malaysia

Abstract—In this study, an inverse microwave scattering model for sea ice has been developed for the purpose of sea ice thickness retrieval using radar backscatter data. The model is loosely based on the Radiative-Transfer-Thermodynamic Inverse Model for Sea Ice Thickness Retrieval from Time-Series Scattering Data. The developed inverse model is a combination of the Radiative Transfer Theory with Dense Medium Phase and Amplitude Correction Theory (RT-DMPACT) forward model and the Levenberg-Marquardt Optimization algorithm. Using input data from ground truth measurements carried out in Ross Island, Antarctica, together with radar backscatter data extracted from purchased satellite images, the sea ice thickness of an area is estimated using the inverse model developed. The estimated sea ice thickness is then compared with the ground truth measurement data to verify its accuracy. The results have shown good promise, with successful estimation of the sea ice thickness within ± 0.15 m of the actual measurement. A theoretical analysis has also revealed that the model faces difficulty once the sea ice thickness exceeds 1.7 m. This can be considered in the future development and improvement of the model.

Received 4 October 2010, Accepted 25 November 2010, Scheduled 17 December 2010
Corresponding author: Yu Jen Lee (leeyj@utar.edu.my).

1. INTRODUCTION

Studies have shown a close relationship between global climate change and changes in the Antarctic ice sheets, which affect the complex interactions of the ecosystem and sea water levels. In a report by the Antarctic and Southern Ocean Coalition (ASOC) at the 30th Antarctic Treaty Consultative Meetings (ATCM), the presence of high ice sheets in the Antarctic makes it a powerful heat sink that strongly affects the climate of the Earth. Next, the white surface of the snow and sea ice also reflects 90% of the sun's radiation, while the sea ice cover modulates exchanges of heat, moisture and gases between the atmosphere and ocean. Lastly, as sea ice forms during the winter, the rejected salt sinks to the sea floor, forming the Oxygen-rich Antarctic Bottom Water that flows North under the world's oceans.

Recent events, such as the collapse of the Larsen B Ice Shelf and the retreat of the Northern Larsen Ice Shelf in Antarctica, as reported by Rack and Rott at the 16th International Workshop of the Forum for Research on Ice Shelf Processes in 2002 at Bergen, Norway and the observed new record low of 4 million km^2 of the Arctic sea ice extent in September 2007, as reported by the Intergovernmental Panel on Climate Change (IPCC) has further reinforced the urgency of studying the impact of global climate change on the polar region, its current severity as well as to find ways to observe global climate change through the monitoring of the ice sheets in the polar region.

The use of microwave remote sensing for data collection and monitoring of the sea ice in the polar region seems convenient and efficient. However, prior to that, the development of forward models to understand the scattering mechanisms by the different properties of snow and sea ice is needed [1, 2]. Then, based on these scattering models, the development of practical methods of inverting observed remote sensing data into proper information on sea ice can be done [3]. There is a substantial amount of existing work on inverse scattering algorithms for the reconstruction of sea ice physical properties from backscatter data. One important parameter being looked into is the sea ice thickness. Thickness information of the sea ice is essential towards the understanding of the dynamics of sea ice cover and the heat exchange between the ocean and the atmosphere, which in turn is crucial towards the study of global climate change.

Inverse algorithms for sea ice thickness retrieval based on a combination of the Radiative Transfer Theory, the Thermodynamic Ice Growth Model and the Levenberg-Marquardt Optimization Algorithm has been proposed [4–6]. The models use time-series electromagnetic scattering data to retrieve sea ice thickness. While these methods

have proven successful in retrieving the thickness of lab grown ice, it has yet to be tested under actual conditions. In addition, time-series measurements using satellites can also be time consuming and costly.

The use of neural networks for the inversion of the mean thickness of young sea ice has also been reported [7]. This model uses data sets of the scattering coefficients of the sea ice generated using a scattering model to train the neural network so that the network is able to give an estimation of the sea ice thickness. This technique has shown consistency in inverting sea ice thickness within a range of 6–9 cm. Yet, sea ice in the polar region can grow to several metres thick. In addition, the paper also reports a failure to retrieve thickness at lower incident angles.

Another existing method is the Reflectivity Inversion for Sea Ice Thickness, based on the influence of the sea ice thickness on the reflectivity properties of the saline ice. [8] explained these properties using a surface backscattering model. Sea ice thickness retrieval is then done by comparing the measured reflectivity with the calculated reflectivity using reflectivity equations as a function of the sea ice thickness. It is found that when the thickness is over one wavelength, sea ice thickness can be inverted directly from reflectivity measurements. However, this method was only tested on very thin sea ice about 20 cm thick.

One more inversion technique mentioned in [3] is the use of proxy indicators of sea ice thickness. Proxy indicators are alternative properties of the sea ice that has a measurable electromagnetic signature and is related to the sea ice thickness. Among the proxy indicators proposed are: ice type and ice age, surface roughness, dielectric properties and ice surface temperature. While these proxy indicators have shown promise in sea ice thickness inversion, they have also been found to demonstrate varying weaknesses under different circumstances.

Finally, there has also been reported work that uses semi-empirical models to estimate sea ice thickness. The objective of the method is to formulate an empirical formula that best describes the sea ice thickness in relation to any other measurable parameters based on the plotted graphs containing these parameters. [9–11] presented some of their works of estimating sea ice thickness, albeit for various purposes, using their own empirical models. This technique however requires large quantities of data in order to formulate an empirical function and the fluctuation and noise that occurs in measurable parameters under actual conditions may cause direct inversion of the sea ice thickness to be difficult.

Therefore, there is still a need to develop better inverse models

for sea ice thickness inversion. Such improvements can be either modifications made to existing models or a proposal of a totally new technique.

2. RADIATIVE TRANSFER INVERSE SCATTERING MODEL (RTISM)

In this paper, a new inverse model for sea ice thickness retrieval based on the Radiative Transfer theory is presented. The inverse model is called the Radiative Transfer Inverse Scattering Model (RTISM) for Sea Ice Thickness Retrieval. This new model is based loosely on the Radiative Transfer-thermodynamic Inverse Model for Sea Ice Thickness Retrieval from Time-series Scattering Data. The original model consists of: the Radiative Transfer forward model, an ice growth model and the Levenberg-Marquardt Optimization Algorithm. The literature study reports that this proposed model has been successfully tested on laboratory grown saline ice sheets using time-series electromagnetic measurement data carried out at the U.S. Army Cold Regions Research and Engineering Laboratory (CRREL) [12, 13].

While the model has shown success, there are several shortcomings reported by the literature. First, the testing of the model has not yet been done on actual conditions in the polar region so far. As the ice sheet is grown artificially, much of the data required for thickness retrieval are already known prior to the simulation, while in real conditions, some data may not be readily available. In addition, time-series satellite remote sensing data retrieval can be tedious, difficult and also very expensive. Lastly, the study reports that most of the thickness retrieval is done on very thin ice that is less than 20 cm thick [14]. In the polar region, the sea ice can grow up to 3–4 m.

The newly proposed inverse model aims to explore the possibility of retrieving sea ice thickness under actual conditions without the use of time-series electromagnetic backscatter data. Therefore, several modifications were made on the original model to adapt to the study objectives and available data. Firstly, the original forward model was replaced with an improved forward model, the RT-DMPACT Forward Model. Next, the Saline Ice Growth Model was omitted as the parameters collected from the field measurements carried out for this study are not time-series data. A detailed flow chart of the Radiative Transfer Inverse Scattering Model for Sea Ice Thickness Retrieval is shown in Figure 1.

The RT-DMPACT Forward Model utilizes the Radiative Transfer Theory incorporated with the Dense Medium Phase and Amplitude Correction Theory (DMPACT). The forward model considers the sea

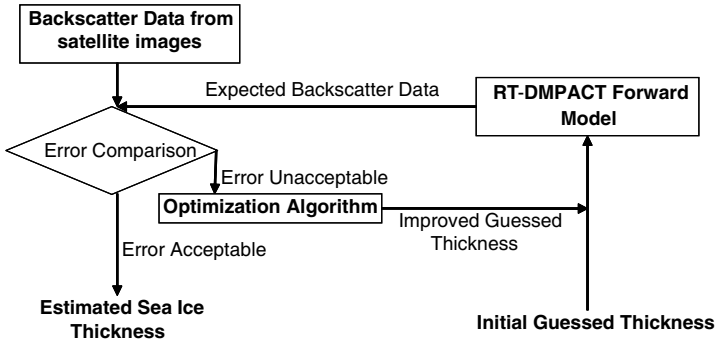

Figure 1. RT-DMPACT inverse scattering model for sea ice thickness retrieval flowchart.

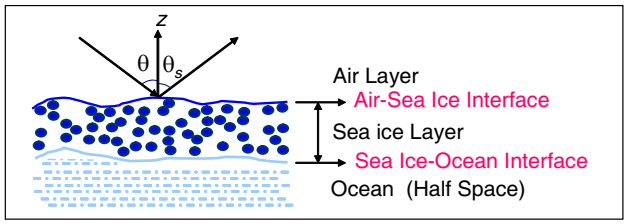

Figure 2. Model configuration for the RT-DMPACT single layer forward model.

ice as an electrically dense media [15]. This forward model provides the relationship between the sea ice characteristics and the radar backscatter data. The configuration for the forward model is shown in Figure 2. The configuration given is for single layer only, while θ and θ_S are defined as the angle of propagation of the incident and scattered wave, respectively.

The classical formulation of the Radiative Transfer Theory used to calculate the propagation and scattering of microwave of a specific intensity in a particular medium is given by:

$$\cos\theta \frac{\partial I}{\partial z} = -\bar{\bar{\kappa}}_e \bar{I} + \int \bar{\bar{P}} \bar{I} \partial\Omega \tag{1}$$

where I, k_e, P, $d\Omega$ and z are the Stokes vector, extinction matrix, phase matrix of the medium, solid angle and vertical direction, respectively [16, 17]. The scattering and absorption loss of the Stokes vector along a propagation direction have been taken into account by the extinction matrix.

The phase matrix, P, from Equation (1) has the following

expression:

$$\bar{\bar{P}}\left(\theta,\phi;\theta',\phi'\right) = \left\langle |\psi|^2 \right\rangle_n \cdot \bar{\bar{S}} = \begin{bmatrix} P_{vv} & P_{vh} \\ P_{hv} & P_{hh} \end{bmatrix} \tag{2}$$

where $\left\langle |\psi|^2 \right\rangle_n$ is the dense medium phase correction factor and S is the Stokes matrix for Mie scatterers with Close Spacing Amplitude Correction that relates the scattered intensities to the incident intensities of the scatterer [18, 19].

Since the sea ice is considered as an electrically dense medium, the dense medium phase correction factor, $\langle |\psi|^2 \rangle_n$ from Equation (2), is incorporated into the phase matrix to take into account the close spacing effect or coherent effect of scattering among the scatterers, thus giving a more accurate result. This factor can be further expressed as:

$$\begin{aligned} \left\langle |\Psi|^2 \right\rangle_n &= \frac{1 - e^{-k_{si}^2\sigma^2}}{d^3} + \frac{e^{-k_{si}^2\sigma^2}}{d^3} \sum_{q=1}^{\infty} \frac{(k_{si}^2\sigma^2)^q}{q!} \\ &\quad \cdot \left[\left(\sqrt{\frac{\pi}{q}} \left(\frac{l}{d} \right) \right)^3 \exp\left(\frac{-k_{si}^2 l^2}{4q} \right) - a\left(k_x\right) a\left(k_y\right) a\left(k_z\right) \right] \end{aligned} \tag{3}$$

where σ^2 represents the variance of the positions of the scatterers, k is the propagation vector, d is the average distance between scatterers, l is the correlation length and $a(k_\gamma)$ is given by:

$$a\left(k_r\right) = \sqrt{\frac{\pi}{q}} \left(\frac{l}{d} \right) \exp\left(\frac{-k_r^2 l^2}{4q} \right) \mathrm{Re}\left\{ \mathrm{erf}\left(\frac{(qd/l) + jk_r l}{2\sqrt{q}} \right) \right\} \tag{4}$$

where erf() is an error function that provides approximation for some of the terms in the noncoherent component of the phase correction factor. The DMPACT was developed by generalizing the concept of the standard antenna array concept. A more detailed formulation and analysis of the DMPACT is given in [18, 20].

During the calculation process, the Radiative Transfer equation is first converted from a differential equation into an integral equation, where the equation is then solved iteratively by including boundary conditions. The detailed derivation for solving the Radiative Transfer equation can be found in [21, 22]. The Integral Equation Method (IEM) is integrated into the forward model to calculate the backscattering effects between the air-snow interface, snow-sea ice interface and sea ice-ocean interface. A detailed formulation of the above method is given by [23]. The detailed iterative solution of a backscatter model integrating the Radiative Transfer equation, DMPACT and IEM can be found in [24]. The output from the forward model will be the backscatter data for co- and cross-polarization (σ_{HH}, σ_{HV}, σ_{VH}, σ_{VV}).

The Levenberg-Marquardt Optimization Algorithm provides a numerical solution to the nonlinear RT-DMPACT Forward Model function. It was chosen over a variety of optimization techniques [25], due to its robustness and flexibility. The algorithm operates to optimize the parameters β of a model curve $f(x_i, \beta)$ from a set of empirical data pairs consisting of both independent and dependent variables, (x_i, y_i), so that the sum of squares of the deviations, $S(\beta)$, becomes minimal [26]. The sum of squares of the deviations, $S(\beta)$, is given by the following expression:

$$S(\beta) = \sum_{i=1}^{m} [y_i - f(x_i, \beta)]^2 \tag{5}$$

where y_i and $f(x_i, \beta)$ represent the radar backscatter data obtained from the satellite images (σ'_{HH}, σ'_{HV}, σ'_{VH}, σ'_{VV}) and the solution of the forward model (σ_{HH}, σ_{HV}, σ_{VH}, σ_{VV}), respectively. β represents the sea ice thickness while x_i represents the other variables involved in solving the forward model. Equation (5) thus becomes:

$$S(\beta) = \sum_{i=1}^{m} \left[\sigma - \sigma'\right]^2 \tag{6}$$

The algorithm's minimization process is initiated by an initial guess on β. During the iteration process, β is replaced by $\beta + \delta$. δ is determined through the approximation of the functions $f(x_i, \beta + \delta)$ by their linearizations as shown below:

$$f(x_i, \beta + \delta) \approx f(x_i, \beta) + J_i \delta, \tag{7}$$

where the gradient of f with respect to β is given by

$$J_i = \frac{\partial f(x_i, \beta)}{\partial \beta}. \tag{8}$$

During the optimization, the solution of the forward model is utilized to construct the Jacobian matrix. Equation (8) then becomes:

$$J_i = \frac{\partial \sigma'}{\partial \beta} \tag{9}$$

At the minimum of the sum of squares, where it is denoted by S, the gradient of S with respect to β is equivalent to 0. Utilizing the above first-order approximation of $f(x_i, \beta + \delta)$ to differentiate S and then setting the result to zero, the function for determining δ can be represented by the following expression:

$$\delta = \left(J^H J + \lambda I\right)^{-1} J^H [y - f(\beta)], \tag{10}$$

where J represents a Jacobian matrix with i rows that equals J_i; J^H is the transposed Jacobian matrix J, where 'H' denotes the Hermitian operator for complex conjugate transpose; λ is the damping factor; I is the identity matrix and f and y are the vectors with ith component $f(x_i, \beta)$ and y_i, respectively. A more detailed solution can be found in [27].

In the developed inverse algorithm, the Levenberg-Marquardt Optimization Algorithm is utilized to reduce the deviation between the forward model output backscatter data and the radar backscatter data obtained from the satellite images by adjusting the sea ice thickness value during each iteration process. While the damping factor, λ, influences the performance of the optimization, our simulations with varied λ showed little impact on the retrieval. An extension of the study to look into this may be done for future work.

2.1. Radar Backscatter Data Extracted from Satellite Images

Satellite images are ordered every year during the preparation of the ground truth measurement to Ross Island, Antarctica. The images are usually acquired a few days before the field trip to ensure the landscape is in its natural state during satellite imaging. For co-polarized radar backscatter data, the RADARSAT-1 satellite image was acquired every year from 2002–2007. For 2008 however, due to the unavailability of RADARSAT-1, a RADARSAT-2 satellite image was instead acquired. The specifications for both RADARSAT-1 and RADARSAT-2 are presented in Table 1.

In the next section, some information regarding the ground truth measurement, such as the objectives, collected data, measurement equipment and measurement procedures will be explained.

Table 1. Specifications for RADARSAT-1 and RADARSAT-2.

	RADARSAT-1	**RADARSAT-2**
Instrument	SAR	SAR
Operating Band	C-Band	C-Band
Polarization	HH	HH/HV
Beam Mode	Standard 2	Standard 2
Resolution	20 m × 27 m	20 m × 27 m
Incidence Angle	24°–31°	24°–31°

3. GROUND TRUTH MEASUREMENT

Ground truth measurements had been carried out in areas around Ross Island, Antarctica over a period of 8 years since 2001. There are several objectives in carrying out the ground truth measurement. Firstly, it is to obtain ground data for the purpose of validating the developed model [28]. In addition, the data are also utilized as part of a long-term observation study on the variation of the parameters over a period of years.

3.1. Location of the Ground Truth Measurement

The ground truth measurement was carried out in areas around Ross Island, Antarctica in collaboration with Antarctica New Zealand (ANZ), who offered logistical support as well as accommodation at their Antarctica base in Ross Island (Scott Base). Sites were selected from these areas and measurements were then carried out at these sites. Figure 3 shows a map of Antarctica with the location of Ross Island and a map of Ross Island itself.

For the purpose of the study, three main terrains have been identified as measurement areas during the field trip, namely the ice shelf, the multi year sea ice and the first year sea ice. As travelling in Antarctica could be cumbersome and time consuming only areas

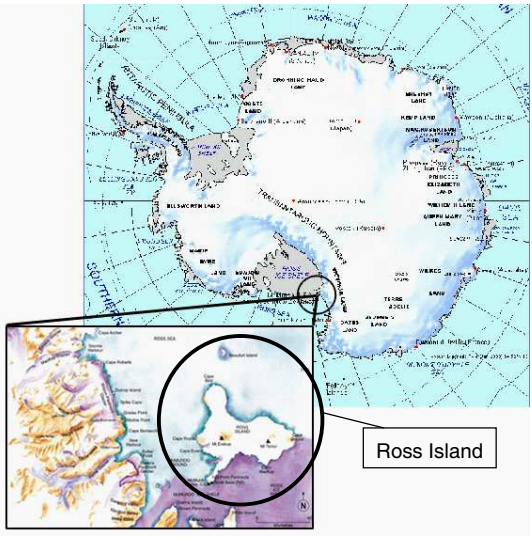

Figure 3. Map of Antarctica and Ross Island.

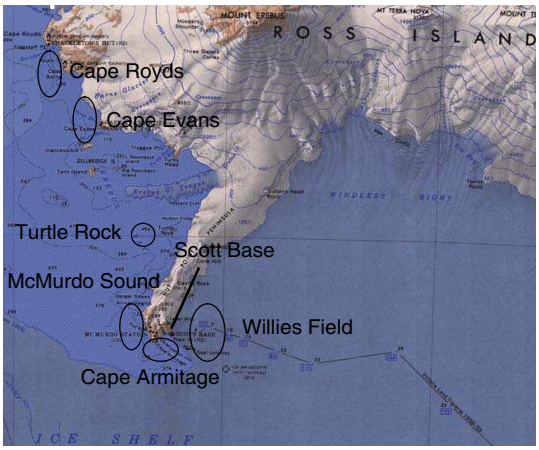

Figure 4. Map showing the areas visited during the ground truth measurement.

within half a day's drive from Scott Base were selected for the purpose of data collection. For the ice shelf, measurements were carried out in sites selected at areas near Willies Field. For the multi year sea ice, measurements were carried out at sites selected in areas near Scott Base, McMurdo Sound, Cape Armitage and Turtle Rock. Finally, for first year sea ice, measurements were carried out at sites selected in areas near Cape Evans up to Cape Royds. A detailed map of the areas visited during the ground truth measurement trips since 2001 is shown in Figure 4.

Cape Royds is the farthest location from Scott Base that was visited during the ground truth measurement. It took about half a day just to reach Cape Royds before any measurements could be carried out. As a result of its location, there had been a couple of years where the planned trips to this area had been cancelled due to poor weather conditions. Luckily however, there are alternative first year sea ice areas. First year sea ice measurements could still be carried out at Cape Evans and at the icebreaker route along McMurdo Sound.

3.2. Data Collection for Ground Truth Measurement

The data collected upon arrival at the site chosen are the site location coordinates, time, date, snow and sea ice surface profile; air, snow and sea ice temperature; snow and sea ice thickness; ocean salinity and temperature and finally the collection of snow and sea ice samples for further processing to obtain other parameters.

Some of the data obtained from the ground truth measurement were either measured or calculated at Scott Base. These parameters were obtained from the processing of the snow and sea ice samples collected from the measurement sites. The parameters that were retrieved were the solid weight and volume of the sea ice; the liquid weight and volume of both the snow and sea ice, the calculation of the solid density for the sea ice and the liquid density for both the snow and sea ice; the snow and sea ice salinity; and lastly the photographing of the cut sea ice sample that showed the sea ice bubble and brine.

Some of the data used for the project were acquired through calculation using models and equations in the literature. Parameters such as dielectric properties of the snow, sea ice and ocean were obtained based on empirical models discussed in [22]. From the photographs showing the surface roughness profile of the snow and sea ice, further image processing was done to obtain the RMS height and correlation length [29]. The scatterer size, distribution and volume of the sea ice were estimated from the photographs of the sea ice slice taken using Matlab. In the next section, the findings and results for the study shall be presented.

4. MULTIYEAR MEASUREMENT AND RETRIEVAL RESULTS

In this section, the findings are presented in several sections. Firstly, a sensitivity analysis done using the RT-DMPACT Single Layer Forward Model on first year sea ice is presented. Next, the multiyear measurement analysis of the parameters collected from first year sea ice and one particular multiyear sea ice measurement site visited every year during the ground truth measurement are discussed. Then, a thorough investigation of the limitations and applicability of the developed inverse model over a range of conditions is discussed. Finally, the actual retrieval of sea ice thickness using the inverse model using ground truth measurement data is presented.

4.1. Sensitivity Analysis

In this section, the influence and sensitivity of various parameters on radar backscatter data was explored using the RT-DMPACT Single Layer Forward Model. This study shall focus only on first year sea ice by varying one parameter over a range of values while keeping the other parameters constant. The generated backscatter data from the forward model was then used to plot graphs in relation to the particular parameter. This study was done using the average values of

Table 2. Model configuration for the RT-DMPACT single layer forward model.

Operating Frequency (GHz)	5.3	
Incidence Angle (°)	25	
Sea Ice Thickness (m)	1.7	
Volume Fraction of Sea Ice (%)	3.5	
Scatterer Radius (mm)	0.4	
Top Layer Dielectric Constant (Air)	1.00	0.00
Scatterer Permittivity (Brine)	40.13	35.15
Background Layer Dielectric Constant (Sea Ice)	3.53	1.19E-2
Bottom Layer Dielectric Constant (Ocean)	59.02	43.51
Top Surface RMS Height and Correlation Length (m)	4.99E-3	5.54E-3
Bottom Surface RMS Height and Correlation Length (m)	2.8E-4*	2.1E-2*

Note: * denotes estimated values based on [21].

the first year sea ice measurements collected from 2005–2007. Table 2 summarizes the fixed first year sea ice when they were not varied. The operating frequency and incidence angle for most of the simulations except for the first (where frequency is varied) and second case (where incidence angle is varied) are fixed at 5.3 GHz and 25°, respectively.

4.1.1. Operating Frequency

The influence of the operating frequency of the satellite on the backscattering coefficient of first year sea ice was first studied. In this simulation, the operating frequency was varied from 0.5 GHz to 10 GHz in intervals of 0.5 GHz with the incidence angle set at 25°. The reason that this range was chosen is to cover common operating frequencies of the various satellites currently in orbit that are used for remote sensing applications. Figure 5 shows the plotted graph of the backscattering coefficients of first year sea ice for the various frequencies.

From this analysis, it is observed that the backscattering coefficient for co-polarization is generally higher than that of the cross-polarization throughout all the operating frequencies. Next, the

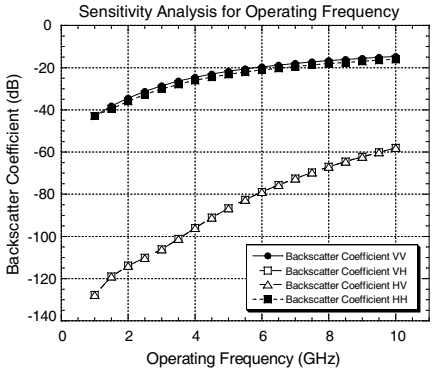

Figure 5. Sensitivity analysis for operating frequency from 1 GHz to 10 GHz.

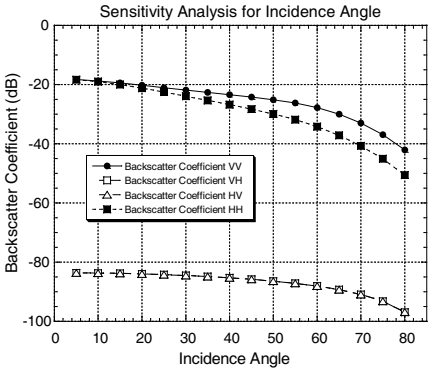

Figure 6. Sensitivity analysis for incidence angle from 5° to 80°.

backscatter coefficients for the two co-polarized fields are comparable. From the graph, as the operating frequency increases, the backscatter coefficients for all fields gradually increase as well.

Although the backscattering coefficient increases as the frequency becomes higher, yet, higher frequency backscattering coefficient data may not be that desirable for parameter retrieval. This is because the penetration capability of the wave needs to also be taken into account. Generally, the penetration depth of the wave decreases when the frequency of the wave increases. Based on the above analysis, the use of the RADARSAT and ENVISAT satellite data, both operate at 5.3 GHz, can be used for the retrieval of first year sea ice thickness not more than 2 m. The influence of the incidence angle on the backscattering coefficient shall be discussed in the next subsection.

4.1.2. Incidence Angle

In this subsection, the influence of the variation in the incidence angle of the electromagnetic wave is presented. For this analysis, the simulation was done by varying the incidence angle from 5° to 80° in intervals of 5°. Figure 6 shows the plotted graph of the backscattering coefficients of first year sea ice for the various incidence angles.

From this analysis, it is observed that the backscattering coefficient for both co-polarizations drop as the incidence angle is increased. The backscattering coefficient data for HH polarization is observed to be generally slightly lower than that of VV polarization. Also, the difference between both polarizations is smaller at lower

incidence angles with increasing difference at higher incidence angles. For cross polarization, both sets of backscattering coefficients appear to be consistently the same.

The study shows that the more desirable range of incidence angles for the study for better wave penetration through layer of sea should be at the lower incidence angles up to about 40°. The satellite data that are acquired for this study usually contain an incidence angle range between 20° to 35°, which falls in the above mentioned incidence angle range as well. In the next subsection, the sensitivity of the backscatter coefficient towards variations in the sea ice thickness shall be looked into.

4.1.3. Sea Ice Thickness

The main purpose of the development of the inverse model is to retrieve sea ice thickness using microwave remote sensing data. In order for the inverse model to be successful, the forward model must be sensitive towards the changes in the sea ice thickness. In order to test the sensitivity of the backscatter coefficient towards sea ice thickness, the sea ice thickness was varied during the simulation from 0.2 m to 2 m in intervals of 0.1 m. Figure 7 shows the plotted graph of the backscattering coefficients of first year sea ice for the various sea ice thicknesses.

From the simulation, the resulting graph shows that the backscattering coefficient for all polarizations drops as the sea ice thickness increases. The drop in both the co-polarized backscattering coefficients are quite high for very thin sea ice with thickness of up to about 0.5 m, where the changes become very small after that,

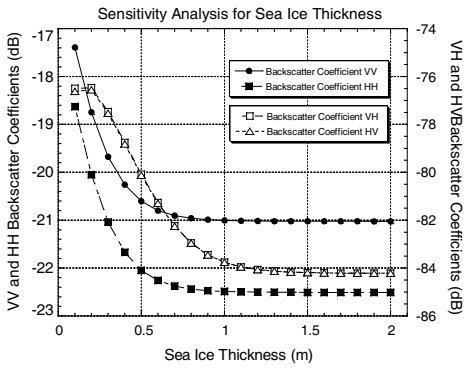

Figure 7. Sensitivity analysis for sea ice thickness from 0.1 m to 2 m.

causing the plotted graph to appear almost constant as the sea ice thickness increases up to 2 m. For the cross polarization backscattering coefficient, the variation is quite high as the sea ice thickness increases up to about 1 m, in which the changes also become smaller thereafter.

From this case study, it can be concluded that while it is possible to use co-polarized backscattering data alone during the parameter retrieval, problems may still occur for thicknesses of sea ice from 0.7 m to 2 m as the backscattering coefficient data saturate. The same trend is observed for cross-polarization data for thicknesses of sea ice from 1.1 m to 2 m. This analysis shows that when the thickness increases until the attenuation of the microwave is too large for it to reach the bottom of the sea ice layer, the backscatter radar returns saturate and thus the retrieval of sea ice thickness becomes difficult for larger thickness of sea ice. Therefore there is no guarantee that parameter retrieval using a combination of both co- and cross-polarized data may be better than just a single type of data. For this study, focus shall remain on utilizing co-polarized data for the sea ice thickness retrieval first rather than utilizing all four polarization data.

In the next section, the multiyear measurements of first year sea ice and multiyear sea ice are presented. The measurement results shall cover ground truth measurements from the years 2002 to 2008.

4.2. Multiyear Measurement Analysis

In this section, the multiyear measurements for first year sea ice and multiyear sea ice are presented. "Multiyear measurement" in this paper refers to a series of measurements over a number of years (2001 to 2008) at the Antarctica sites. For first year sea ice, the average values of the collected data from Cape Evans were used for the analysis. As for the multiyear sea ice, the measurements from the repeated site near Cape Armitage at coordinates 166°43'E and 77°51'S were utilized. The analysis for first year sea ice covered ground truth measurement data from the years 2005 to 2008, where 2005 was the first year measurements were conducted at first year sea ice areas. For the multiyear sea ice, the analysis covered the ground truth measurement data from the year 2002 to 2008.

The multiyear measurement analysis was performed to find out the variations of the parameters of the actual sea ice in Ross Island, Antarctica over the years. The analysis allows the study of which of the parameters had little variation throughout the years and thus, can be eliminated as unknown variables during the development of the inverse model. Next, the measurement data includes the sea ice thickness, which may be useful towards the study of climate change. Lastly,

research can also be done to relate how the surrounding environment influences the change in the parameters.

4.2.1. Ocean Dielectric Constant

The ocean dielectric constant is usually used as the bottom layer dielectric constant during the simulation of the inverse model for first year sea ice. Figure 8 shows the calculated dielectric constant of the ocean for first year sea ice from 2005 to 2008 while Figure 9 shows the calculated dielectric constant of the ocean for multi year sea ice 2002 to 2008. Both calculations were done at a frequency of 5.3 GHz.

From the graphs, it is observed that the calculation of the dielectric constant using both the ocean temperature and salinity had remained almost constant over the years for both first year and multiyear sea ice, due to the influence of both parameters, which also remained virtually constant over the years and varied little. It can be concluded that the ocean dielectric constant is quite constant and can therefore be treated not as a variable during the development of the inverse model.

4.2.2. Snow and Sea Ice Thickness

The thickness of the snow and sea ice plays an important role as an indicator of global climate change. Normally, during the ground truth measurement, snow cover can be observed for multiyear sea ice sites as the snow from these areas are thicker and have yet to begin melting.

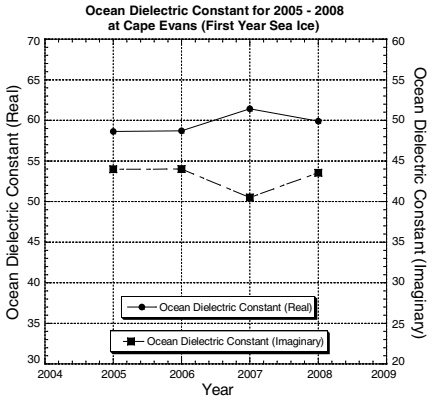

Figure 8. Multiyear calculation of the ocean dielectric constant for first year sea ice.

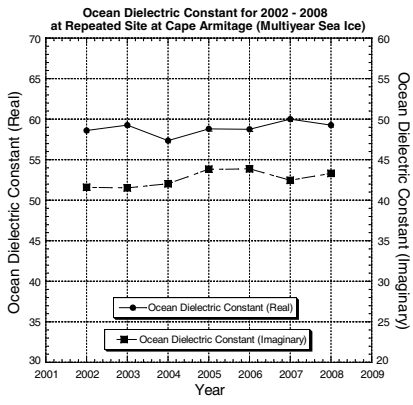

Figure 9. Multiyear calculation of the ocean dielectric constant for multiyear sea ice.

This scenario however, is not found in first year sea ice areas as the snow cover in these areas have usually melted by the time of the ground truth measurement. As such, the snow cover for these areas are usually very thin (less than 10 cm thick) or non-existent. Figure 10 presents the sea ice thickness from 2005 to 2008 for first year sea ice while Figure 11 depicts the snow and sea ice thickness from 2001 to 2008 for multiyear sea ice.

For the first year sea ice, it is observed that the thickness dropped slightly before gradually increasing. The data shown in this graph is the average of the sea ice thickness measurement for all the sites at Cape Evans for each year and thus, may not be as accurate as measuring in a geographically same site every year. While the measurements are consistent and fall within the usual range of less than 2 m, for 2008, the sea ice thickness measured was more than 2 m and the highest so far.

From Figure 11, it is observed that both the snow and sea ice thickness gradually increased from 2001 to 2004. This increase was most probably caused by the blocking of the B-15A Iceberg near Ross Island that occurred during 2002, causing the sea ice to slowly pile up. There was a significant drop for both the snow and sea ice thickness during 2005 as it was reported that the iceberg had drifted away sometime in 2004, thus allowing fresh sea water to flow into the Ross Island area again. Since then, the thickness for sea ice at the repeated site had remained quite constant, but the snow thickness instead had showed a gradual increase.

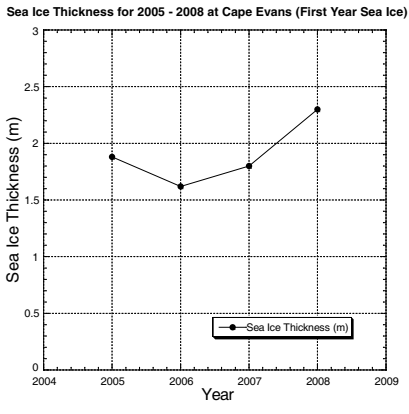

Figure 10. Multiyear measurement of the sea ice thickness for first year sea ice.

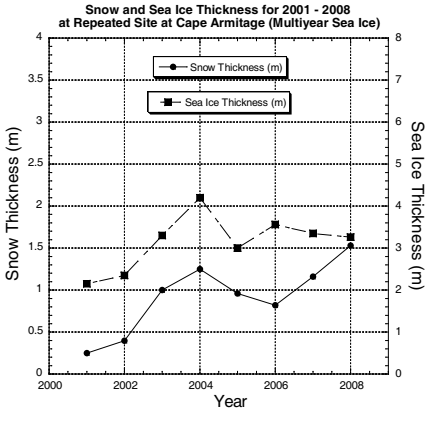

Figure 11. Multiyear measurement of the snow and sea ice thickness for multiyear sea ice.

4.2.3. Dielectric Constant of Snow and Sea Ice

The dielectric constants of the snow and sea ice are some of the important input parameters during the sea ice thickness retrieval using the inverse model. Figure 12 shows the calculated dielectric constant of snow for the multiyear sea ice repeated site. The calculation was done by treating the snow as dry snow due to the extreme cold weather in Antarctica. The frequency used for calculation was 5.3 GHz. Then, Figures 13 and 14 present the calculated dielectric constant of sea ice for both first year and multiyear sea ice. These calculations were made by taking the frequency to be 5.3 GHz. The snow dielectric constant shows small changes over the period of seven years that the ground truth measurement had been carried out.

For first year sea ice, the sea ice dielectric constant had remained almost constant throughout the four years of measurement. Therefore, it can be assumed that the sea ice dielectric constant for first year sea ice is quite constant and thus can be treated not as a variable during the inversion of the sea ice thickness. The dielectric constant for multiyear sea ice also shows a similar trend when compared to first year sea ice. Both the real and imaginary parts of the sea ice dielectric constant show variations, but on closer inspection, the changes are quite small. Thus, the dielectric constant of multiyear sea ice can also be regarded as a constant during the simulation of the inverse model.

This concludes the multiyear measurement analysis. The next section shall present the theoretical analysis of the developed inverse model to study its limitations and applicability.

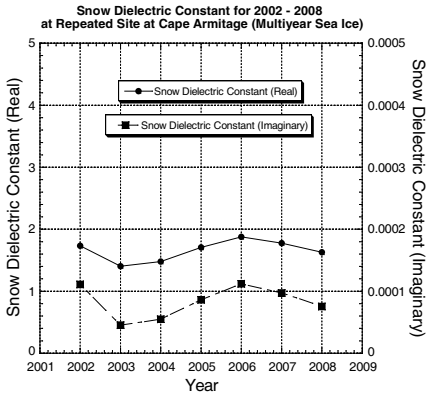

Figure 12. Multiyear calculation of the snow dielectric constant for multiyear sea ice.

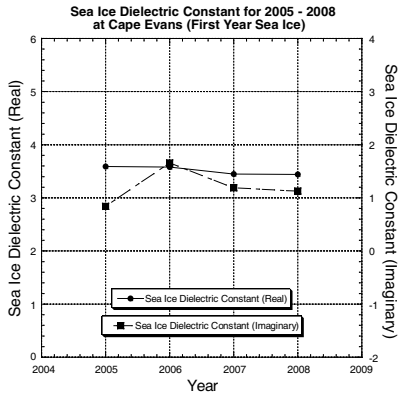

Figure 13. Multiyear calculation of the sea ice dielectric constant for first year sea ice.

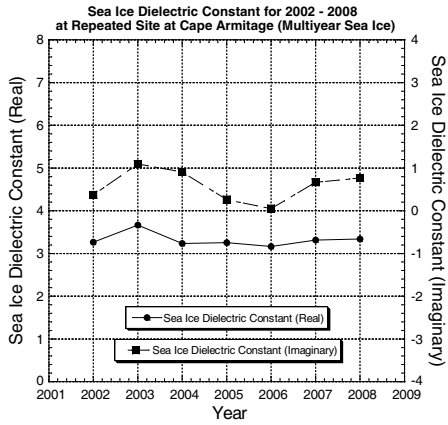

Figure 14. Multiyear calculation of the sea ice dielectric constant for multiyear sea ice.

4.3. Theoretical Analysis of the Radiative Transfer Inverse Scattering Model

In order to understand the performance of the developed inverse model and to find out its limitations during the inversion of the sea ice thickness, several simulations were done. In the first analysis, the ability of the developed inverse model to predict sea ice thickness was tested using a random set of input values. The radar backscatter data used for the comparison were backscatter coefficients obtained through simulation using the forward model with the same set of random inputs. Figure 15 shows the results from the first theoretical analysis of the inverse model.

In the graph, ten results from the first analysis are presented. The inverse model was used to estimate random sea ice thickness ranging from 0.5 m to 5 m for any single frequency from a range of 1 GHz to 10 GHz for each test. Although using only a random set of input parameters, the analysis showed that the developed inverse model was able to function as expected, successfully estimating the sea ice thickness from random initial guesses. However, this test also revealed that the inverse model only works properly up to about 7 GHz for sea ice thickness estimation from 0.5 m to 2 m as the model fails to converge and yield a result when the range above is exceeded. Future study can be conducted to improve this. As the thickness was increased, the process of sea ice parameter retrieval became slower due to fewer changes in the backscattering coefficient, which was barely detected by the program and was critical for the inversion process.

In the second theoretical analysis, the operating frequency and sea ice thickness was varied to see how robust the inverse model is. As opposed to the first analysis which used random parameter values, the parameters used in this investigation were average values of the parameters measured during the ground truth measurement for different years. Again, the radar backscatter data used for comparison were simulated using the forward model with the same set of parameters used for this analysis for HH polarization and 5.3 GHz.

For this analysis, the tests were configured in the order as follows; 0.2 m sea ice thickness retrieval using 1 GHz, 5.3 GHz and 10 GHz (test number 1, 2 and 3, respectively); 1 m sea ice thickness retrieval using 1 GHz, 5.3 GHz and 10 GHz (test number 4, 5 and 6, respectively) and lastly 1.7 m sea ice thickness retrieval using 1 GHz, 5.3 GHz and 10 GHz (test number 7, 8 and 9, respectively), which are altogether nine cases. This was to simulate retrieval for young sea ice, first year sea ice and multiyear sea ice (with no snow cover on top of it) using different frequencies. Figure 16 depicts the results from the second theoretical analysis.

In Figure 16, the results of the eight successful tests out of nine mentioned previously are shown. It is found that the inverse model is able to estimate the sea ice thickness for 0.2 m using frequencies at 1 GHz, 5.3 GHz and 10 GHz. The tests also revealed that the range of initial guesses for the successful inversion for very thin sea ice is about ± 0.15 m from the actual thickness before converging to final estimated values. The accuracy of the prediction for very young sea ice using the model was about ± 0.1 m.

Next, the model is able to successfully predict the sea ice thickness

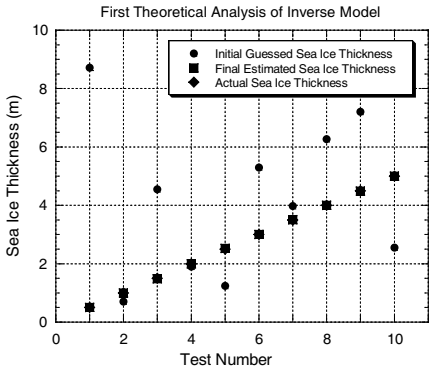

Figure 15. First theoretical analysis of the radiative transfer inverse scattering model.

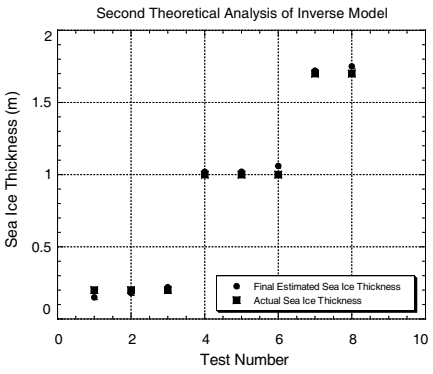

Figure 16. Second theoretical analysis of the radiative transfer inverse scattering model.

for 1 m at 1 GHz, 5.3 GHz and 10 GHz. The simulation also shows that the range of initial guesses for the successful inversion for first year sea ice at 1 m is about ± 0.2 m from the actual thickness. The accuracy of the prediction for 1 m thick first year sea ice was about ± 0.1 m.

Lastly, the model is able to successfully predict the sea ice thickness for 1.7 m at 1 GHz and 5.3 GHz. The accuracy of the prediction for first year sea ice is about ± 0.15 m. The results also show that inversion for sea ice thickness at 1.7 m at 10 GHz is difficult. This is because the model program detects the differences in the simulated backscatter coefficient and improves the thickness guess accordingly. For 10 GHz, the change in the backscatter is almost negligible for the different thickness between 1 m to 2 m, thus making it impossible for an accurate guess.

As a conclusion, the analysis revealed that the inverse model should only be used for the retrieval of either very young or first year sea ice thickness and not for multiyear sea ice with thickness thicker than 2 m. Due to this, the retrieval should also generally utilize low frequency data between 1 GHz to 5.3 GHz. In the next section, the results of the actual sea ice thickness retrieval using the inverse model on ground truth measurement sites shall be discussed.

4.4. Sea Ice Thickness Retrieval for Ground Truth Measurement Sites

In this section, the results of the inverse model to retrieve sea ice thickness using actual ground truth measurement data for the years 2005 to 2007 on first year sea ice are presented. The reason only first year sea ice was chosen for this analysis is because the absence or lack of snow in first year sea ice sites allows the terrain to match the model configuration of the single layer forward model implemented in the inverse model. Next, the testing was performed only after 2005 because the ground truth measurements on first year sea ice only began in 2005.

The radar backscatter data used as the comparison data for the inverse model during the retrieval process were the actual radar backscatter data extracted from the RADARSAT-1/-2 satellite images. For this study, only RADARSAT-1/-2 backscatter data was utilized as the acquisition of this satellite image was complete from the years 2005 to 2008. Therefore, the simulations only used HH polarization radar backscatter data for the inversion of the sea ice thickness. Also, the inversions were made by setting the input frequency as 5.3 GHz and incidence angle as 25°, which is the configuration for the RADARSAT-1/-2 satellite images. Next, the average values from the multiyear measurements for parameters such as dielectric constant for ocean, sea

ice, top surface roughness and volume fraction are utilized. For bottom surface roughness the estimated value in Table 2 was used. Figure 17 shows the sea ice thickness retrieval for sites in the year 2005.

In 2005, only three first year sea ice sites were visited, where one site was at Cape Royds and the other two were at Cape Evans. Using the developed inverse model, the sea ice thickness for the three sites were estimated and compared with the actual ground truth measurement data. The results show acceptable matching between both sets of data as the difference between the predicted and actual sea ice thickness was not more than 4 cm. The next figure shows the sea ice thickness retrieval for sites in the year 2006.

In 2006, five first year sea ice sites were visited, where two sites were at Cape Royds and the other three were at Cape Evans. The graph shows good matching between both the estimated and actual measured sea ice thickness, with differences of not more than 4 cm between both sets of data.

In Figure 19, the estimation results for the sea ice thickness for 2007 are shown. The inversion of the sea ice thickness for 2007 was also considered successful, with the difference of only 5 cm between the actual and predicted sea ice thickness. However, there was only one set of data for this year because during the day of the ground truth measurement to the first year sea ice sites, the weather was bad and the measurement trip had to be cut short. This concludes the analysis of the sea ice thickness retrieval using actual ground truth measurement data utilizing the developed inverse model.

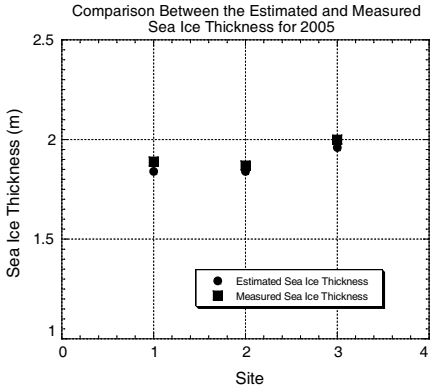

Figure 17. Comparison between the estimated and measured sea ice thickness for 2005.

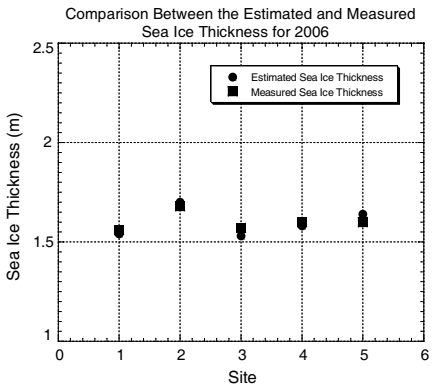

Figure 18. Comparison between the estimated and measured sea ice thickness for 2006.

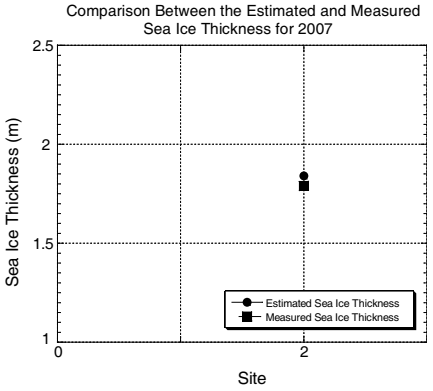

Figure 19. Comparison between the estimated and measured sea ice thickness for 2007.

5. CONCLUSION AND FUTURE WORK

As a conclusion, an inverse model for the retrieval of sea ice thickness has been developed. Preliminary tests of the inverse model for the retrieval of sea ice thickness under actual conditions in the Antarctic have shown promising results, with good agreements achieved between the model estimations and actual sea ice thickness. However, the use of the model to predict sea ice thickness more than 2 m should be done cautiously as the model showed difficulty in thickness predictions when the sea ice becomes very thick. In future works, the model will be extended to include inversion based on full polarization data from the satellite images. The current single layer forward model incorporated might be extended to a multilayer model. The study may also be extended to allow inversion of other sea ice physical parameters other than sea ice thickness.

REFERENCES

1. Golden, K. M., M. Cheney, K. H. Ding, A. K. Fung, T. C. Grenfell, D. Isaacson, J. A. Kong, S. V. Nghiem, J. Sylvester, and D. P. Winebrenner, "Forward electromagnetic scattering models for sea ice," *IEEE Transactions on Geoscience and Remote Sensing*, Vol. 36, No. 5, 1655–1674, 1998.
2. Liang, D., P. Xu, L. Tsang, Z. Gui, and K.-S. Chen, "Electromagnetic scattering by rough surfaces with large heights

and slopes with applications to microwave remote sensing of rough surface over layered media," *Progress In Electromagnetics Research*, Vol. 95, 199–218, 2009.

3. Golden, K. M., D. Borup, M. Cheney, E. Cherkaeva, M. S. Dawson, K. H. Ding, A. K. Fung, D. Isaacson, S. A. Johnson, A. K. Jordan, J. A. Kong, R. Kwok, S. V. Nghiem, R. G. Onstott, J. Sylvester, D. P. Winebrenner, and I. H. H. Zabel, "Inverse electromagnetic scattering models for sea ice," *IEEE Transactions on Geoscience and Remote Sensing*, Vol. 36, No. 5, 1675–1704, 1998.
4. Veysoglu, M. E., H. T. Ewe, A. K. Jordan, R. T. Shin, and J. A. Kong, "Inversion algorithms for remote sensing of sea ice," *International Geoscience and Remote Sensing Symposium (IGARSS), Vol. 1: Surface and Atmospheric Remote Sensing: Technologies, Data Analysis and Interpretation*, 626–628, 1994.
5. Shih, S. E., K. H. Ding, S. V. Nghiem, C. C. Hsu, J. A. Kong, and A. K. Jordan, "Thickness retrieval using time series electromagnetic measurements of laboratory grown saline ice," *International Geoscience and Remote Sensing Symposium (IGARSS), Vol. 2: Remote Sensing for a Sustainable Future*, 1208–1210, 1996.
6. Shih, S. E., K. H. Ding, S. V. Nghiem, C. C. Hsu, J. A. Kong, and A. K. Jordan, "Saline ice thickness retrieval using time series c-band polarimetric radar measurements," *IEEE Transactions on Geoscience and Remote Sensing*, Vol. 36, No. 5, 1589–1598, 1998.
7. Kwok, R., S. V. Nghiem, S. H. Yueh, and D. D. Huynh, "Retrieval of thin ice thickness from multifrequency polarimetric SAR data," *Remote Sensing of Environment*, Vol. 51, 461–474, 1995.
8. Fung, A. K. and R. G. Onstott, "Modeling of ice thickness effect and its application to data interpretation," *International Geoscience and Remote Sensing Symposium (IGARSS), Vol. 2: Remote Sensing for a Sustainable Future*, 1202–1204, 1996.
9. Pfaffling, A., C. Haas, and J. E. Reid, "Empirical inversion of hem data for sea ice thickness mapping," *Extended Abstracts, 10th European Meeting of Environmental and Engineering Geophysics (EAGE's Near Surface 2004)*, A037, Utrecht, The Netherlands, 2004.
10. Hendricks, S., C. Haas, S. Gobell, and J. Haapala, "Laser and radar (LaRa) surface elevation retrieval and ice thickness measurements in the baltic sea," *European Geosciences Union General Assembly*, poster paper, Vienna, April 2006.
11. Ji, Y., J. Zhang, and J. Meng, "ABMR ice thickness model and its

applications to bohai sea in China," *Progress In Electromagnetics Research*, Vol. 76, 183–194, 2007.

12. Nghiem, S. V., R. Kwok, S. H. Yueh, A. J. Gow, D. K. Perovich, J. A. Kong, and C. C. Hsu, "Evolution in polarimetric signatures of thin saline ice under constant growth," *Radio Science*, Vol. 32, No. 1, 127–151, 1997.
13. Golden, K. M., M. Cheney, K. H. Ding, A. K. Fung, T. C. Grenfell, D. Isaacson, J. A. Kong, S. V. Nghiem, J. Sylvester, and D. P. Winebrenner, "Forward electromagnetic scattering models for sea ice," *IEEE Transactions on Geoscience and Remote Sensing*, Vol. 36, No. 5, 1655–1674, 1998.
14. Shih, S. E., K. H. Ding, S. V. Nghiem, C. C. Hsu, J. A. Kong, and A. K. Jordan, "Saline ice thickness retrieval using time series C-band polarimetric radar measurements," *IEEE Transactions on Geoscience and Remote Sensing*, Vol. 36, No. 5, 1589–1598, 1998.
15. Albert, M. D., T. E. Tan, H. T. Ewe, and H. T. Chuah, "A theoretical and measurement study of sea ice and ice shelf in antarctica as electrically dense media," *Journal of Electromagnetic Waves and Applications*, Vol. 19, No. 14, 1973–1981, 2005.
16. Chandrasekhar, S., *Radiative Transfer*, Dover, New York, 1960.
17. Ulaby, F. T., R. K. Moore, and A. K. Fung, *Microwave Remote Sensing, Active and Passive: Vol. 1. Microwave Remote Sensing Fundamentals and Radiometry*, Addison-Wesley Publishing Company, Massachusetts, 1981.
18. Chuah, H. T., S. Tjuatja, A. K. Fung, and J. W. Bredow, "A phase matrix for a dense discrete random medium: Evaluation of volume scattering coefficient," *IEEE Transactions on Geoscience and Remote Sensing*, Vol. 34, No. 5, 1137–1143, 1996.
19. Fung, A. K. and H. J. Eom, "A study of backscattering and emission from closely packed inhomogeneous media," *IEEE Transactions on Geoscience and Remote Sensing*, Vol. 23, No. 5, 761–767, 1985.
20. Ewe, H. T. and H. T. Chuah, "An analysis of the scattering of discrete scatterers in an electrically dense medium," *1998 IEEE International Geoscience and Remote Sensing Symposium Proceedings (IGARSS'98)*, Vol. 5, 2378–2380, July 6–10, 1998.
21. Fung, A. K., *Microwave Scattering and Emission Models and Their Applications*, Artech House, Norwood, 1994.
22. Ulaby, F. T., R. K. Moore, and A. K. Fung, *Microwave Remote Sensing, Active and Passive: Vol. 3, From Theory to Applications*, Addison-Wesley Publishing Company, Massachusetts, 1986.

23. Fung, A. K., Z. Li, and K. S. Chen, "Backscattering from a randomly rough dielectric surface," *IEEE Transactions on Geoscience and Remote Sensing*, Vol. 30, No. 2, 356–369, 1992.
24. Ewe, H. T., H. T. Chuah, and A. K. Fung, "A backscatter model for a dense discrete medium: Analysis and numerical results," *Remote Sensing of Environment*, Vol. 65, No. 2, 195–203, 1998.
25. Madsen, K., H. B. Nielsen, and O. Tingleff, *Methods for Non-linear Least Squares Problems*, Lecture Notes, 2nd Edition, Informatics and Mathematical Modelling, Technical University of Denmark, DTU, Lyngby, 2004.
26. Gill, P. E. and W. Murray, "Algorithms for the solution of the nonlinear least-squares problem," *Journal of Society for Industrial and Applied Mathematics*, Vol. 15, No. 5, 977–992, 1978.
27. Marquardt, D. W., "An algorithm for least-squares estimation of non-linear parameters," *Journal of Society for Industrial and Applied Mathematics*, Vol. 11, No. 2, 431–441, 1963.
28. Winebrenner, D. P., L. Tsang, B. H. Wen, and R. West, "Sea ice characterization measurements needed for the testing of microwave remote sensing models," *IEEE Journal of Oceanic Engineering*, Vol. 14, No. 2, 149–158, 1989.
29. Ulaby, F. T., R. K. Moore, and A. K. Fung, *Microwave Remote Sensing, Active and Passive: Vol. 2, Radar Remote Sensing and Surface Scattering and Emission Theory*, Addison-Wesley Publishing Company, Massachusetts, 1982.